

The Effect of Post-Growth Annealing on the Physical Properties of Fe-Doped ZnO Nanostructure

Qadir Bakhsh Yasir

PhD research fellow at Hohai University, China

Email address: qadirkhsh.yasir@gcu.edu.pk

Dr. Barkat Ali Laghari

Associate Professor of Physics

GC University Hyderabad

Email address: dr.barkatali.laghari@gcu.edu.pk

Muhammad Asif

PhD research fellow at Hohai University, China

Email address: asifphy123@gmail.com

Dr. Mazhar Ali Abbasi

Professor of Physics at the Institute of Physics University of Sindh Jamshoro

email address: mazharabbasi@usindh.edu.pk

Hong Bing Yao

Professor of Physics at Hohai University China

email address: alenyao@hhu.edu.cn

Abdul Sajid

PhD research fellow at Karachi University & Lecturer, Dept: of Physics, GC University Hyderabad

Email address: abdul.sajid@gcu.edu.pk

Dr. Muhammad Najam Shaikh

Assistant Professor, Department of Physics, GC University Hyderabad

Email: dr.muhammadnajam.shaikh@gcu.edu.pk

ABSTRACT

The synthesis of nanostructure materials for optoelectronic and photonic devices is often scrutinized. Due to its reasonable and environmentally benign nature, ZnO, a semiconductor, is well regarded for its potential to develop photonic devices. In this respect, low-temperature aqueous chemical growth is used to create ZnO nanostructures doped with Fe. The temperature-dependent change in the Fe-doped ZnO nanostructure was seen in the XRD spectra at larger angles (200°C, 400°C, 600°C). It was shown that the crystalline size of as-grown Fe-doped ZnO nanostructures grows in correlation with a reduction in the d-spacing value. Furthermore, U-V visible spectroscopy measurements are conducted for all the synthesized samples. It is also observed from the U-V visible spectroscopy measurements that the energy band gap of the Fe-doped ZnO decreases by increasing the Fe concentration. We investigate the influence of post-growth annealing on the energy gap of the sample with 5% Fe content and find that increasing the temperature reduces the energy gap.

The SEM results revealed that hexagonal rods like nanostructure are successfully synthesized for pure ZnO whereas no morphological change occurred for Fe doped ZnO. Moreover, the destroyed surface after annealing was identified inside the SEM particles. This research will help to develop LEDs due to decrease in band gap.

Keywords: ZnO, Nanostructures, Fe, annealing, morphology

1: INTRODUCTION

"Nano" is a small term but has enormous promise and has had a huge effect on the fields of engineering and science. Richard Feynman coined the term "nanotechnology" in 1959, under the caption "There is plenty of room at the bottom," to describe its revolutionary potential [1]. Professor Norio Taniguchi of a Japanese scientific institution introduced nanotechnology in 1974, and it has progressed beyond the pioneering stage and established itself in the scientific community as a reputable study [2]. Nanotechnology is based on exceedingly small scales and has developed rapidly over the years [3]. Devices for observing surface images at atomic level e.g., Atomic Force Microscope (AFM), Scanning Electron Microscope (SEM) etc. are widely used [4]. The Royal Society defined two terms, Nanotechnology and Nanoscience which describes the properties of material at atomic and molecular level which are different from normal behavior of material [5]. In 2001, the European Commission established the definition of nonmaterial as a material that may be natural, identical, or manufactured material containing particles in an unbound state [6]. Nanoparticles have unique physical and chemical characteristics; they have a greater surface area to volume ratio than their bulk counterparts. Zero, one, two, and three dimensional structures may be found in nanostructures [7,8]. Nanostructures [9-12] are 1-dimensional (e.g., Nanotubes), 2-dimensional (e.g., Thin films) and 3-dimensional (e.g., Nanostructures with dimensions greater than 100nm). Nanomaterials can be synthesized to change their properties by changing their particle size [13]. Due to large area to volume ratio, it can be used to achieve diverse results [14]. Nanomaterials have unique optical properties in biomedicine, solar cells etc. These can be detected after doping [15]. Nanomaterials have excellent electronic properties which are useful for electronic equipment. E.g., Ferroelectric nanoparticles are useful in liquid crystal displays [16, 17]. Nanomaterials have a significant role in mechanical aspect of device applications. E.g., assessment of nano-mechanical stability, explicit strength with substrate [18]. Nanomaterials can also play a vital role in the energy sector. Zinc oxide can be widely used in manufacturing nano-generators and lithium particles batteries [19-21]. Electrical and magnetic properties of Zinc oxide can be enhanced drastically by doping it with Iron. Moreover, it has an impact on absorbance, band gap, and transmittance [22-24]. But it does not affect the hexagonal wurtzite's shape. Due to its bactericidal and antibacterial properties, zinc oxide particles lose their

structure [25]. Nanostructures of zinc oxide are essential in electronics, photonics, and optics. Zinc oxide has an energy gap of 3.37 eV and an excitation binding energy of 60 meV at room temperature [26]. It is mostly used to create semi-conducting materials due to its uniqueness like piezoelectric materials [27], transparent conductors [28], chemical sensors [29], tiny wavelength light emitting devices [30, 31], and gratzel-type solar cells [32] etc. Some of the numerous nanostructures that can be made using diverse techniques include nanocones, nanostars, nanoflowers, nano-crystallites, nanobeads, nanotubes, nanocages, nanoscale pyramids, organically capped nanocrystals, nanobelts, nanorods, and nanowires [33,34]. Spray pyrolysis was used to produce ferric oxide (Fe_2O_3) at temperatures between 300 and 500 degrees Celsius and field emission scanning electron microscopy (FESEM) was used to examine the surface of annealed Fe_2O_3 nanostructures [35]. An amazingly simple technique to fabricate nanostructured ZnO for chemical sensors by Vardan Galstyan et al. [36]. Zinc oxide has a high bandgap and is a semiconductor so it can be doped with different ions. Due to its hexagonal wurtzite structure, zinc oxide is vital for a variety of uses. Energy gaps are frequently impacted by doping and annealing. However, it is important to explore the effect of doping and annealing in this research process. This could be done by employing the simple aqueous chemical growth procedure. We aim to study the effects of doping at different percentages on zinc oxide with iron, investigate the effects of annealing on the surface morphology of zinc oxide with iron doping using SEM, and observe annealing effects on transmittance using UV visible and crystal structure by using XRD.

2: RESEARCH METHODOLOGY

2.1 MATERIALS USED IN THIS RESEARCH:

Chemicals: For this study, we utilized chemicals purchased from a company called "Dae-Jung Chemicals," which were used exactly as they were sold to us (no mixing). Success in this study depends on the use of iron, zinc nitrate, hexamethylenetetramine, and deionized water.

Samples Preparation:

The hydrothermal growth method was used for preparation of pure zinc oxide and iron doped samples of various iron percent concentrations because this method is easier and cheaper. This method requires a neat and clean substrate otherwise the nanostructures will not be produced. Thus prior to sample preparation, breakers were washed with isopropanol and also given ultrasonic bath treatment for at least 15 minutes for complete removal of dust and grease. particles. Finally, beakers were dried at room temperature. For

preparation of pure ZnO_2 , a solution of 100ml of DI- H_2O containing $[\text{Zn}(\text{NO}_3)_2]$ and HMT was stirred for 15 minutes and $[\text{Zn}(\text{NO}_3)_2]$ was thoroughly combined with HMT. The solution was transferred to a beaker labelled and covered with aluminum foil for safe transport and storage. For preparation of 5%, 10% and 15% iron doped ZnO_2 , in addition to solution of 100ml of DI- H_2O containing $[\text{Zn}(\text{NO}_3)_2]$, HMT, iron was also combined in mentioned concentration in three separate beakers respectively and stirred for thorough combination for 15 minutes. The solutions were transferred to three separate beakers, labeled, and covered with aluminum foil for safe storage and transport. The solutions were then shifted to an oven preheated to 95 degrees Celsius heated for about five hours and cooled to room temperature. The samples were settled down to the bottom of the substrates and were recovered in powder form and dried for further investigation. XRD, SEM, and UV tests of these samples were conducted for the investigation of structural, crystalline, surface morphology, and optical properties, respectively. The samples were then annealed at 200 °C, 400 °C, and 600 °C for about 5 hours. XRD, SEM, and UV tests were again performed for investigation of any change in structural, crystalline, surface morphology, and optical properties, respectively.

2.2 HYDROTHERMAL GROWTH METHOD

Nanotechnology is gaining popularity rapidly, making it a prime target for studies examining both its benefits and drawbacks. There will be a plethora of options that come up in a search for "methods," each with its own set of advantages and disadvantages. Hydrothermal growth is the most well-known and straightforward of the available ways. All the scientists in the world are busy trying to invent new technologies. The recycling of trash, for example, is bad for the planet's inhabitants as well as other things. As a consequence, this strategy is widely used since it consistently yields positive outcomes. The simplicity and low cost of this approach are two major benefits. It is beneficial to the world since it operates at low temperatures and may be used to manufacture a wide variety of useful products. The optoelectric materials may be used in the fabrication of nanomaterials. This approach is used to synthesize iron-doped zinc oxide in this study.

3. RESULTS AND DISCUSSION

This study took advantage of Nanoscale technology and its applications. Zinc oxide semiconductor was chosen because of its special attribute of being one-dimensional.

3.1 X-RAY DIFFRACTION (XRD) ANALYSIS

An analytical X-pert PRO diffractometer produced with CuK α rays having a wavelength of 1.5421 \AA in sum in the apparatus operated together with 30mA at 40 KV was used to examine a range of metal oxide x-ray diffraction spectra in semiconductor materials.

3.1.1 XRD OF PURE ZnO

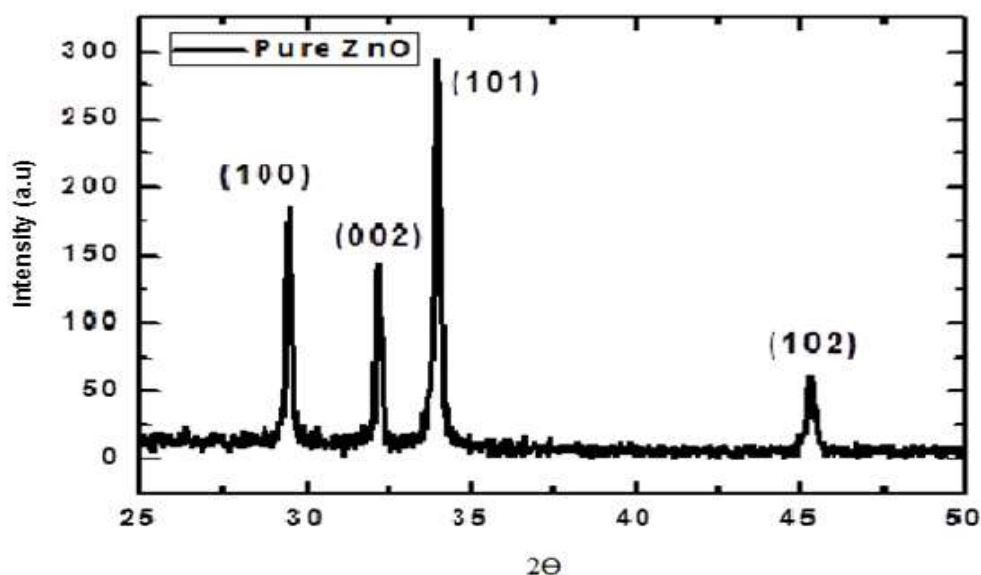


Figure 1: XRD of Pure ZnO

A hexagonal (wurtzite) nanostructure of zinc oxide was created as a sample. The most intense value found in the XRD spectrum was for peak intensity (101), with peak (one hundred) coming in second. Zinc oxide with a nanostructure is growing in importance and is becoming a need in contemporary society. There are no errant peaks in the graph of XRD analysis, it confirms that the sample contains only pure high-quality product ZnO.

3.1.2 Fe DOPED ZnO

Table 1: Concentration of Fe-doped ZnO

CONCENTRATION OF ELEMENTS IN DOPPING					
01	05%	Zinc Nitrate(1.646)gm	HMT (1.05) gm	Distil water (100)ml	Iron(0.082316)gm
02	10%	Zinc Nitrate(1.646)gm	HMT (1.05) gm	Distil water (100)ml	Iron(0.164632)gm
03	15%	Zinc Nitrate(1.646)gm	HMT (1.05) gm	Distil water (100)ml	Iron(0.246948)gm

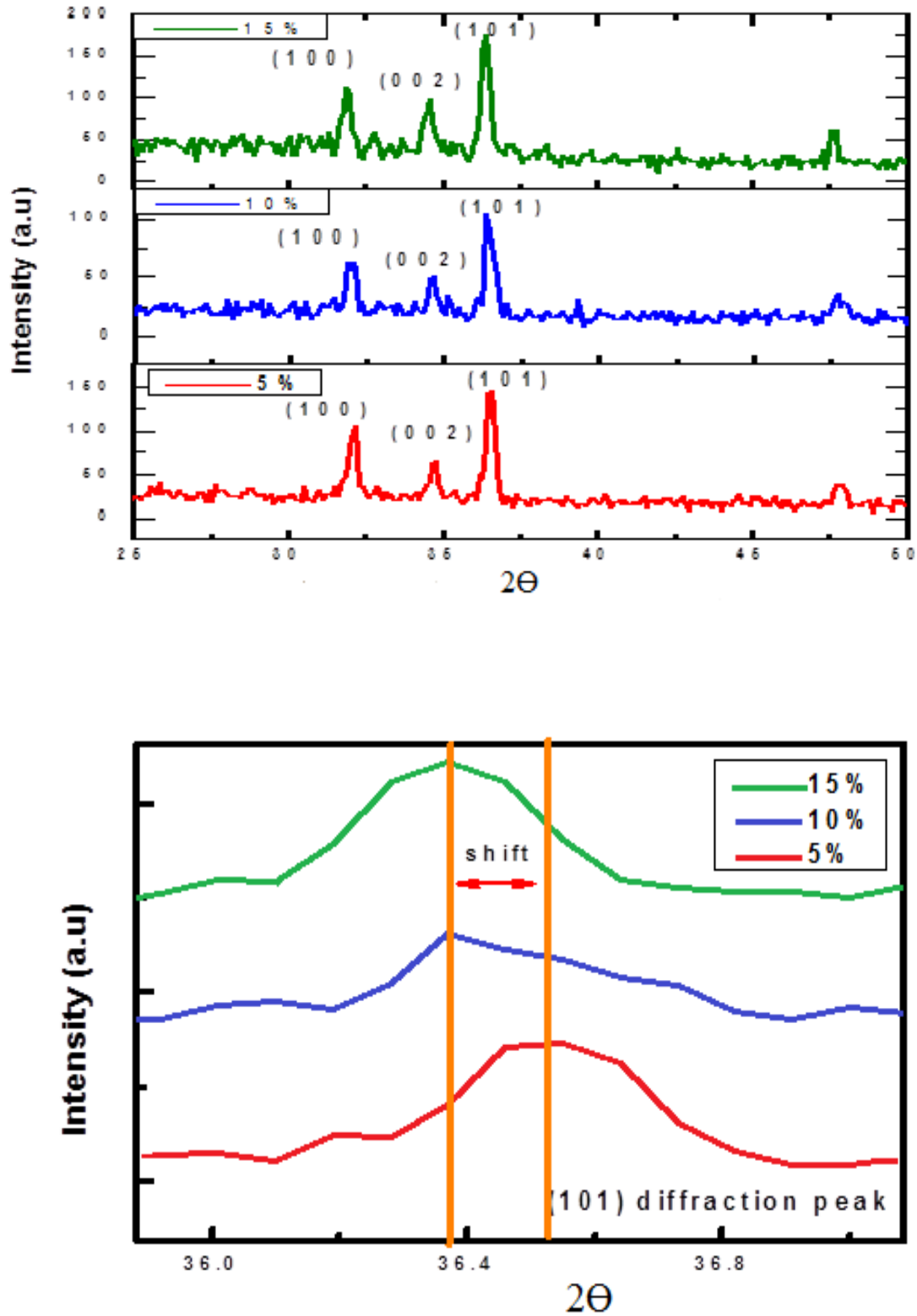
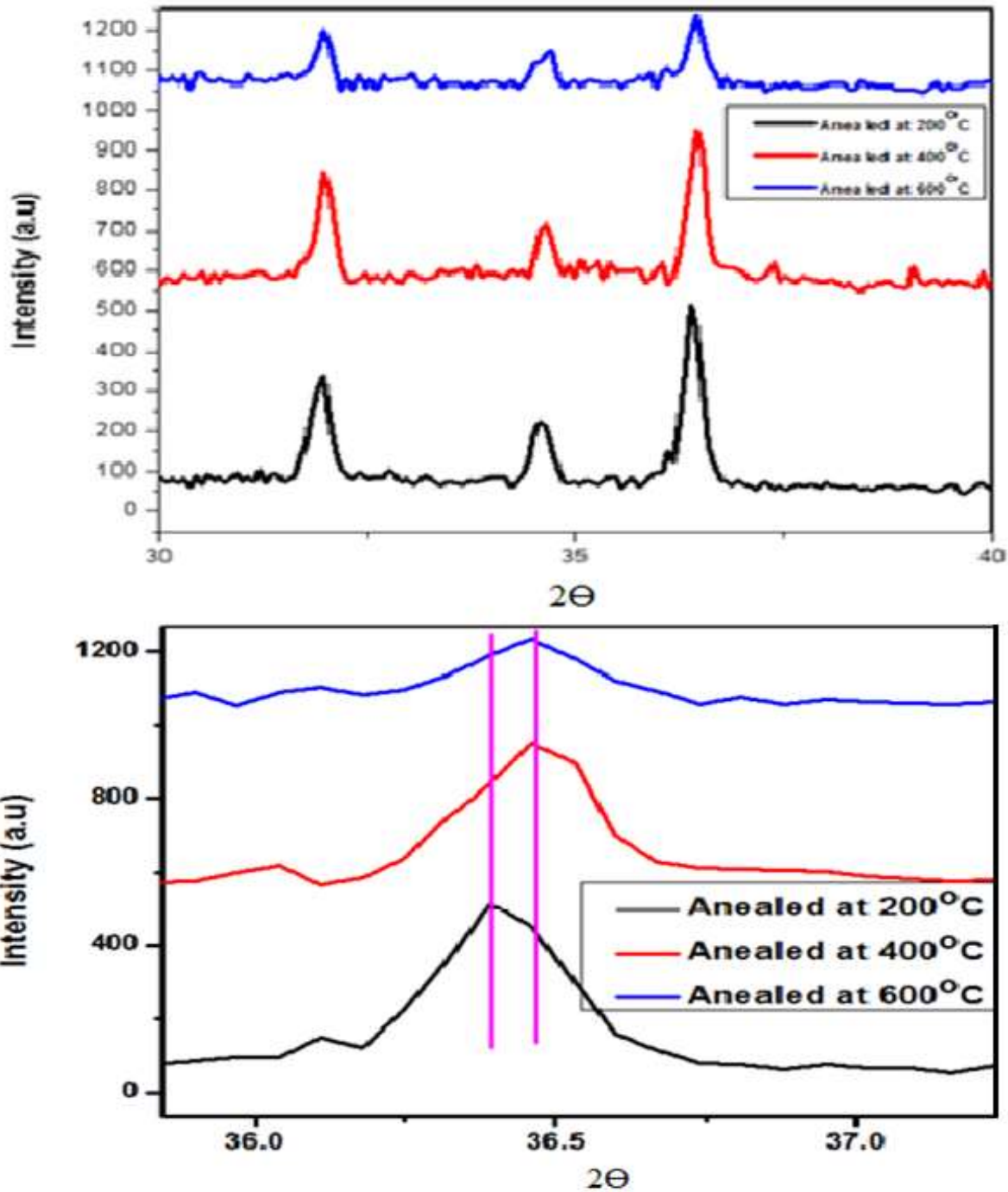


Figure 2: X-Ray Diffraction Spectrum (Fe) iron doped ZnO

To see the behavior of zinc oxide and iron-doped zinc oxide in the graph or XRD spectrum, JCPDS card number 36-1451 is used as support. Three peaks, (one hundred), (002), and last but highest, (101), will be attributed to the form of the hexagonal wurtzite crystal in the graph. When pure zinc oxide is compared to iron-doped zinc oxide in an XRD graph, the peak intensities change. Similarly, it can be seen that when the proportion of doping is raised, diffracted peaks are relocated at smaller angles. With the aid of a graph, it is shown that the value of the d-spacing has grown; the reason for this change is a decrease in the angle's value. Further, the iron-doped zinc oxide peak (101), which is the highest peak, demonstrated that the particle size is within the range of the nanoscale.

3.1.3 ANNEALED Fe DOPED ZnO

Observing the findings of iron-doped zinc oxide nanorods and comparing them to those of annealed iron-doped zinc oxide nanorods reveal that the crystal size and intensity of the (101) peak for zinc oxide nanostructures grow in tandem. As shown by JCPDS card No. 36-1451, the diffraction peaks (one hundred), (002), and (101) in this material may be assigned to the hexagonal wurtzite structure comprised of pure zinc oxide and annealed Iron doped zinc oxide.



Figure

3: Spectrum of Annealed Fe doped ZnO

At 5% Fe doped ZnO, the crystallite size is found to be significantly impacted by the application of several temperature treatments (200°C, 400°C, and 600°C). Moreover, when the temperature rises, all diffraction peaks move in the direction of the high angle. As the peak moves to a greater angle, the d-spacing value drops.

3.1.4 Fe DOPED ZnO NANOSTRUCTURES BEFORE AND AFTER ANNEALING

It has been shown that the wavelength of iron-doped Zinc Oxide nanostructures before and after annealing shifts in the direction of smaller and larger angles, respectively, leading to smaller and larger d-spacing values.

Table 2: Comparative table of XRD test of 5% Fe doped ZnO

Five percent Fe Doped ZnO	Peak positions	FWHM(B)	Crystal Size
As grown	36.531	0.269	77.917
Annealed at 200°C	36.437	0.231	95.183
Annealed at 400°C	36.470	0.218	99.410
Annealed at 600°C	36.4920	0.322	65.721

In comparison to pure zinc doped zinc oxide, iron oxide has a line extending at a diffraction peak (002) that results in nanostructures that are in the range of nano scales. Scherrer's formula [$D = (0.9 \times \lambda) / (d \cos \Theta)$] may be used to calculate the size of the nanostructure crystal of iron doped zinc oxide. It shows that crystalline size of particles increases by increase in temperature but at 600°C it again decreases.

3.2 U.V VISIBLE SPECTRUM (ABSORBANCE) Fe DOPED ZnO

The UV Visible Spectrum of Fe doped ZnO was performed before and after annealing to observe the changes.

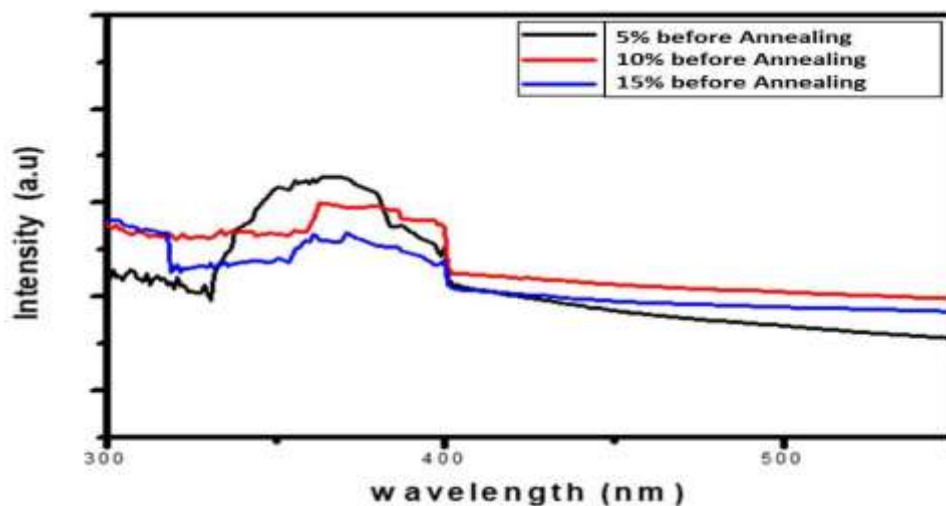


Figure 4: UV-visible spectrum of Fe-doped ZnO Nanostructures before annealing

Table 3: UV-visible spectrum of (absorbance) Fe doped ZnO Nanostructures Before Annealing

S #	Samples	Max: Absorbance at wavelength	Band Gap
01	05% Before annealing	366.6nm	3.40ev
02	Ten percent Before annealing	374.7 nm	3.33ev
03	Fifteen percent Before annealing	385.5 nm	3.240ev

The absorbance spectra of iron-doped zinc oxide are shown in the above graph, and it is clear that there are noticeable shifts in wavelengths. There was a red shift in the spectrum when iron was introduced to zinc oxide nanostructure. As the quantity of dopants increased, there was an increase in the wavelength, and it shifted towards higher values. This led to the observation that the band gap changes along with changes in the doping level. Zinc oxide's band gap narrows when iron is added.

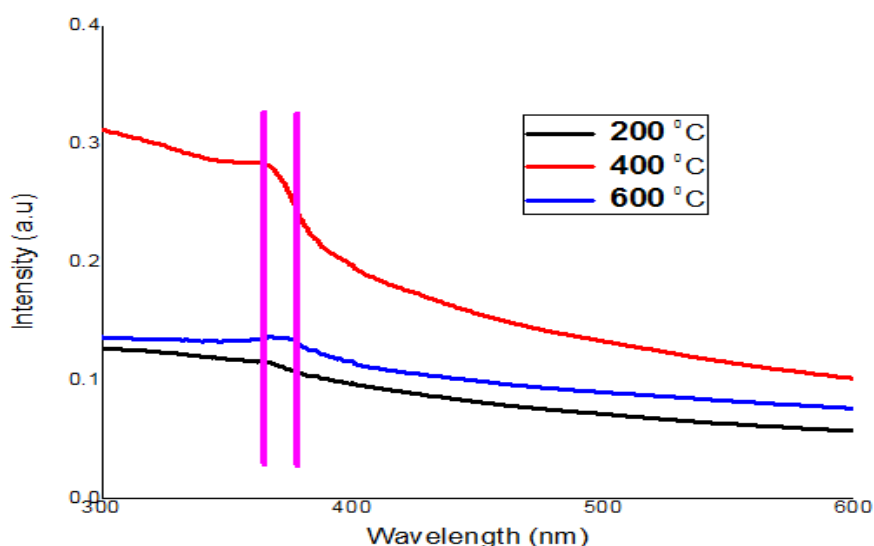


Figure 5: UV-visible spectrum of Fe-doped ZnO Nanostructures after annealing

Table 4: UV-visible spectrum of (absorbance) 5% Fe doped ZnO Nanostructures After Annealing

S #	Annealing temperature	Max: Absorbance at wavelength	Band Gap
01	200°C	368.712nm	3.39ev
02	400°C	365.277 nm	3.42ev
03	600°C	377.989 nm	3.30ev

The absorbance spectra of Fe-doped ZnO after annealing show that the spectra move towards longer wavelengths as the temperature rises which decreases the band gap. Planck's energy equation was used to compute the band gap of annealed samples using the information taken from the spectra mentioned above.

3.3 SEM IMAGES

3.3.1 Fe DOPED ZnO NANOSTRUCTURES BEFORE ANNEALING

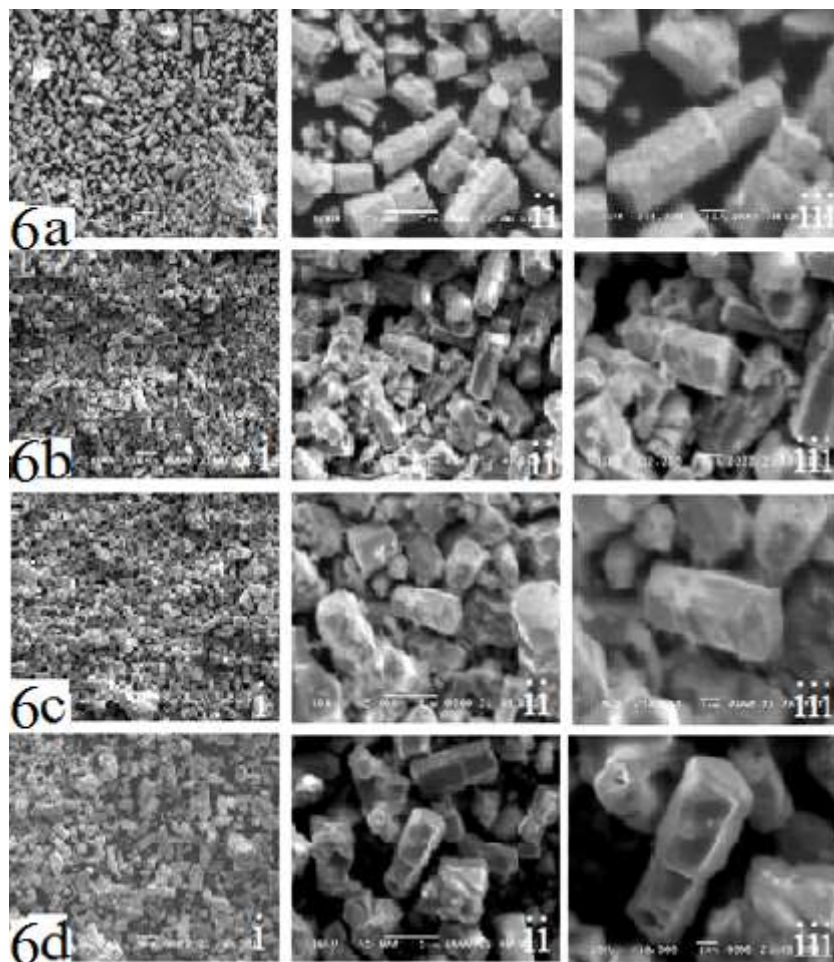


Figure 6(a): SEM images of Pure ZnO, figure 6(b) SEM images of 5% Fe doped ZnO, figure 6(c) SEM images of 10% Fe doped ZnO, figure 6(d) SEM images of 15% Fe doped ZnO.

From figures (6a) before annealing it is observed that at pure zinc oxide Nano-structures have hexagonal rodlike shape. Whereas figure (6b) at 5% Iron doped zinc oxide, behavior of shape is same, but it also shows effect on density as well as on surface texture. On the other hand, 10% doped zinc oxide effect on density and surface morphology which increases as compared to pure and 5% grown Nano-structures. In addition to this figure (6d) at 15% iron doped zinc oxide some modification of surface morphology occurred.

3.3.2 Fe DOPED ZnO NANOSTRUCTURES AFTER ANNEALING

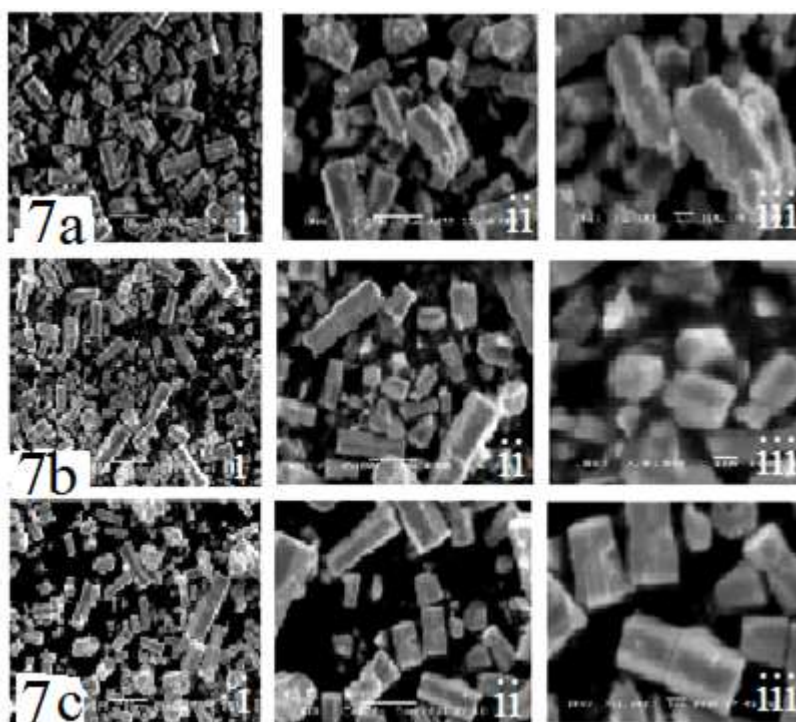


Figure: 7(a) SEM images of 5% Fe doped ZnO annealed at 200°C, figure 7(b) SEM images of 5% Fe doped ZnO annealed at 400°C, figure 7(c) SEM images of 5% Fe doped ZnO annealed at 600°C

The figures (7a, 7b and 7c) are after the annealing. It is observed that at 5% doped zinc oxide at 200°C, 400°C and 600°C due to high temperature the surface of synthesized nanostructures is melting, and its corners are reducing and destroying. Same behavior is observed at all temperatures.

4. CONCLUSION

We determined the crystalline size of the particles using Scherrer's equation. As a result, it increases to 200°C to 400°C and then decreases to 600°C. The XRD spectra revealed that Θ decreased due to increase in doping percentage on and d-spacing value increased but after annealing it reversed, increased and d-spacing value decreased. UV-Visible examinations reveal that as the percentage of doping increases the band gap decreases. Furthermore, after annealing as the temperature increases the band gap again decreases. Scanning electron microscopy is used to examine surface morphology (SEM). According to the current findings, the experimentally developed nanostructures show pure zinc oxide surface morphology to be hexagonal rod-like at low and high magnification, while the result of doping iron with zinc oxide had an impact on density of the nanostructures' surface morphology. Additionally, it has been shown that altering or boosting the iron content

causes agglomeration at the surface of produced nanostructures. This research can help investigate the optical and electrical properties of ZnO by using it in LEDs and semiconducting devices due to the decrease of band gap.

REFERENCE:

- [1] R. P. Feynman, "There's plenty of room at the bottom: An invitation to enter a new field of physics," in *Handbook of Nanoscience, Engineering, and Technology, Third Edition*, ed: CRC Press, 2012, pp. 26-35.
- [2] N. J. Shetty, P. Swati, and K. David, "Nanorobots: Future in dentistry," *The Saudi Dental Journal*, vol. 25, pp. 49-52, 2013.
- [3] R. W. Whatmore, "Nanotechnology—what is it? Should we be worried?," *Occupational Medicine*, vol. 56, pp. 295-299, 2006.
- [4] H. W. Kroto, J. R. Heath, S. C. O'Brien, R. F. Curl, and R. E. Smalley, "C₆₀: Buckminsterfullerene," *Nature*, vol. 318, "p. 162-163", 1985.
- [5] T. Rogers-Hayden and N. Pidgeon, "Moving engagement "upstream"? Nanotechnologies and the Royal Society and Royal Academy of Engineering's inquiry," *Public Understanding of Science*, vol. 16, pp. 345-364, 2007.
- [6] A. K. Bandyopadhyay, *Nanomaterials*: New Age International, 2008.
- [7] L. E. Greene, M. Law, J. Goldberger, F. Kim, J. C. Johnson, Y. Zhang, et al., "Low-temperature wafer-scale production of ZnO nanowire arrays," *Angewandte Chemie International Edition*, vol. 42, pp. 3031-3034, 2003.
- [8] S. Xu and Z. L. Wang, "One-dimensional ZnO nanostructures: solution growth and functional properties," *Nano Research*, vol. 4, pp. 1013-1098, 2011.
- [9] J.-H. Park, H.-J. Choi, Y.-J. Choi, S.-H. Sohn, and J.-G. Park, "Ultrawide ZnO nanosheets," *Journal of Materials Chemistry*, vol. 14, pp. 35-36, 2004.
- [10] M. M. Brewster, M.-Y. Lu, S. K. Lim, M. J. Smith, X. Zhou, and S. Gradecak, "The growth and optical properties of ZnO nanowalls," *The Journal of Physical Chemistry Letters*, vol. 2, pp. 1940-1945, 2011.
- [11] W. Zhao, X. Song, Z. Yin, C. Fan, G. Chen, and S. Sun, "Self-assembly of ZnO nanosheets into nanoflowers at room temperature," *Materials Research Bulletin*, vol. 43, pp. 3171-3176, 2008.
- [12] D. Liu, W. Wu, Y. Qiu, S. Yang, S. Xiao, Q.-Q. Wang, et al., "Surface functionalization of ZnO nanotetrapods with photoactive and electroactive organic monolayers," *Langmuir*, vol. 24, pp. 5052-5059, 2008.
- [13] C. Nützenadel, A. Züttel, D. Chartouni, G. Schmid, and L. Schlapbach, "Critical size and surface effect of the hydrogen interaction of palladium clusters," *The European Physical Journal D*, vol. 8, pp. 245-250, 2000.
- [14] G. C. Bond, C. Louis, and D. T. Thompson, *Catalysis by gold* vol. 6: World Scientific, 2006.
- [15] J. T. Lue, "Physical properties of nanomaterials," *Encyclopedia of nanotechnology*, vol. 10, pp. 1-46, 2007.
- [16] Y. Li, Y. Wu, and B. S. Ong, "Facile synthesis of silver nanoparticles useful for fabrication of high conductivity elements for printed electronics," *Journal of the American Chemical Society*, vol. 127, pp. 3266-3267, 2005.
- [17] S. Kundu, M. Akimoto, I. Hirayama, M. Inoue, S. Kobayashi, and K. Takatoh, "Enhancement of contrast ratio by using ferroelectric nanoparticles in the alignment layer of liquid crystal display," *Japanese Journal of Applied Physics*, vol. 47, pp. 47-51, 2008.
- [18] J. W. Suk, R. D. Piner, J. An, and R. S. Ruoff, "Mechanical properties of monolayer graphene oxide," *ACS nano*, vol. 4, pp. 6557-6564, 2010.
- [19] A. Khan, M. Ali Abbasi, M. Hussain, Z. Hussain Ibupoto, J. Wissting, O. Nur, et al., "Piezoelectric nanogenerator based on zinc oxide nanorods grown on textile cotton fabric," *Applied Physics Letters*, vol. 101, p. 193506, 2012.
- [20] W. J. Beek, M. M. Wienk, and R. A. Janssen, "Efficient hybrid solar cells from zinc oxide nanoparticles and a conjugated polymer," *Advanced Materials*, vol. 16, pp. 1009-1013, 2004.
- [21] W. M. Zhang, J. S. Hu, Y. G. Guo, S. F. Zheng, L. S. Zhong, W. G. Song, et al., "Tin-nanoparticles encapsulated in elastic hollow carbon spheres for high-performance anode material in lithium-ion batteries," *Advanced Materials*, vol. 20, pp. 1160-1165, 2008.
- [22] D. Bagnall, Y. Chen, Z. Zhu, T. Yao, M. Shen, and T. Goto, "High temperature excitonic stimulated emission from ZnO epitaxial layers," *Applied Physics Letters*, vol. 73, pp. 1038-1040, 1998.
- [23] Y. Nakanishi, A. Miyake, H. Kominami, T. Aoki, Y. Hatanaka, and G. Shimaoka, "Preparation of ZnO thin films for high-resolution field emission display by electron beam evaporation," *Applied Surface Science*, vol. 142, pp. 233-236, 1999.
- [24] J. H. Choi, H. Tabata, and T. Kawai, "Initial preferred growth in zinc oxide thin films on Si and amorphous substrates by a pulsed laser deposition," *Journal of Crystal Growth*, vol. 226, pp. 493-500, 2001.
- [25] A. Nahhas, H. K. Kim, and J. Blachere, "Epitaxial growth of ZnO films on Si substrates using an \ epitaxial GaN buffer," *Applied Physics Letters*, vol. 78, pp. 1511-1513, 2001.

- [26] T.-H. Fang and S.-H. Kang, "Preparation and characterization of Mg-doped ZnO nanorods," *Journal of Alloys and Compounds*, vol. 492, pp. 536-542, 2010.
- [27] M. Ghosh and A. Raychaudhuri, "Optical properties of Mg-substituted ZnO nanoparticles obtained by solution growth," *IEEE Transactions on Nanotechnology*, vol. 10, pp. 555-559, 2011
- [28] N. Padmavathy and R. Vijayaraghavan, "Enhanced bioactivity of ZnO nanoparticles—an antimicrobial study," *Science and technology of advanced materials*, vol. 9, p. 035004, 2008.
- [29] Emanetoglu N W, Gorla C, Liu Y, Liang S and Lu Y 1999 *Mater. Sci. Semicond. Process* 2 24.
- [30] D. King and R. Nix, "Thermal stability and reducibility of ZnO and Cu/ZnO catalysts," *Journal of Catalysis*, vol. 160, pp. 76-83, 1996.
- [31] G. Agarwal and R. F. Speyer, "Current change method of reducing gas sensing using ZnO varistors," *Journal of the Electrochemical Society*, vol. 145, pp. 2920-2925, 1998.
- [32] G. T. Rao and D. T. Rao, "Gas sensitivity of ZnO based thick film sensor to NH₃ at room temperature," *Sensors and Actuators B: Chemical*, vol. 55, pp. 166-169, 1999.
- [33] D. S. Ginley and C. Bright, "Transparent conducting oxides," *MRS Bulletin*, vol. 25, pp. 15-18, 2000.
- [34] H. Cao, J. Xu, D. Zhang, S.-H. Chang, S.-T. Ho, E. Seelig, et al., "Spatial confinement of laser light in active random media," *Physical review letters*, vol. 84, p. 5584, 2000.
- [35] D. Bagnall, Y. Chen, Z. Zhu, T. Yao, S. Koyama, M. Y. Shen, et al., "Optically pumped lasing of ZnO at room temperature," *Applied Physics Letters*, vol. 70, pp. 2230-2232, 1997.
- [36] Vardan Galstyan, Elisabetta Comini, Camilla Baratto, Guido Faglia, Giorgio Sberveglieri, "Nanostructured ZnO chemical gas sensors", *Ceramics International*, vol. 41, Issue 10, Part B, pp. 14239-14244, 2015.
- [37] J. Zhong, A. H. Kitai, P. Mascher, and W. Puff, "The influence of processing conditions on point defects and luminescence centers in ZnO," *Journal of the Electrochemical Society*, vol. 140, pp. 3644-3649, 1993.
- [38] C. S. Lao, P. X. Gao, R. S. Yang, Y. Zhang, Y. Dai, and Z. L. Wang, "Formation of double-side teathed nanocombs of ZnO and self-catalysis of Zn-terminated polar surface," *Chemical physics letters*, vol. 417, pp. 358-362, 2006.
- [39] R. Pawar, J. Shaikh, P. Shinde, and P. Patil, "Dye sensitized solar cells based on zinc oxide bottle brush," *Materials Letters*, vol. 65, pp. 2235-2237, 2011.
- [40] Yarub Al-Douri a,b,c,*, Nouredine Amrane d, Mohd Rafie Johan b "Annealing temperature effect on structural and optical investigations of Fe₂O₃ nanostructure. "